Final Draft
of the original manuscript:

Minarik, P.; Jablonska, E.; Kral, R.; Lipov, J.; Ruml, T.; Blawert, C.; Hadzima, B.; Chmelik, F.:

Effect of equal channel angular pressing on in vitro degradation of LAE442 magnesium alloy

In: Materials Science and Engineering C (2016) Elsevier

DOI: 10.1016/j.msec.2016.12.120

Effect of equal channel angular pressing on *in vitro* degradation of LAE442 magnesium alloy

Peter Minárik[1,*], Eva Jablonská[2], Robert Král[1], Jan Lipov[2], Tomáš Ruml[2], Carsten Blawert[3], Branislav Hadzima[4], František Chmelík[1],

[1]*Department of Physics of Materials, Faculty of Mathematics and Physics, Charles University in Prague, Ke Karlovu 5, 121 16 Prague 2, Czech Republic*

[2]*Department of Biochemistry and Microbiology, University of Chemistry and Technology Prague, Technická 5, 166 28 Prague 6, Czech Republic*

[3]*Helmholtz-Zentrum Geesthacht, Zentrum für Material- und Küstenforschung GmbH, Institut für Werkstoffforschung, Max-Planck-Straße 1, Geesthacht, Germany*

[4]*University of Zilina, Univerzitna 8215/1, 010 26 Zilina, Slovakia*

* Corresponding author.

Email address: peter.minarik@mff.cuni.cz, Tel: +420 221 911 360, Fax: +420 221 911 490

Abstract

Effect of processing through equal channel angular pressing (ECAP) on the degradation behaviour of extruded LAE442 magnesium alloy was investigated in 0.1M NaCl solution, Kirkland's biocorrosion medium (KBM) and Minimal essential medium (MEM), both with and without 10% of foetal bovine serum (FBS). Uniform degradation of as extruded and ECAP processed samples in NaCl solution was observed, nevertheless higher corrosion resistance was found in the latter material. Increase of the corrosion resistance due to ECAP was observed also after 14-days immersion in all media used. Higher compactness of the corrosion layer formed

on the samples after ECAP was responsible for the observed decrease of corrosion resistance, which was proved by scanning electron microscope investigation. Lower corrosion rate in media with FBS was observed and was explained by additional effect of protein incorporation on the corrosion layer stability. A cytotoxicity test using L929 cells was carried out to investigate possible effect of processing on the cell viability. Sufficient cytocompatibility of the extruded samples was observed with no adverse effects of the subsequent ECAP processing. In conclusion, this *in vitro* study proved that degradation behaviour of the LAE442 alloy could be improved by subsequent ECAP and this material is a good candidate for future *in vivo* investigation.

Keywords: magnesium; biodegradation; *in vitro*; cytotoxicity; implant material

1 Introduction

Magnesium alloys are nowadays intensively investigated as a potential material for degradable implants [1,2]. Until now, a high number of different Mg alloys have been studied in different *in vitro* and *in vivo* studies [3], from which LAE442 alloy (Mg-4Li-4Al-2RE, wt. %) is one of the most often investigated *in vivo* [4–11]. Relatively low and uniform degradation rate and no negative effect on the surrounding tissue and internal organs makes this alloy to one of the most suitable Mg alloys for orthopaedic applications. Until now, all studies have been conducted on as-cast and extruded material. Comparative *in vivo* studies with as-cast LAE442 alloy showed superior performance compared to other alloys (AZ31, AZ91, WE43) after 18 weeks of implantation period [4,5]. However, gas cavities of evolved H_2 were observed in the surrounding tissue as a result of too rapid degradation rate. Improved *in vivo* degradation behaviour was found in the material after subsequent extrusion. Decrease of the degradation rate and no presence of gas cavities after 12 weeks of implantation period was reported [6]. It

was concluded that grain refinement and homogenization of alloying elements rich secondary phases were responsible for such improvement. Moreover, long-term *in vivo* studies showed superior degradation behaviour of extruded LAE442 alloy after 6 months [7] and 12 months [8] of implantation period in a rabbit model. Furthermore, LAE442 alloy was found to have lower degradation rate than WE43 alloy, which is currently considered as one of the most promising ones. The WE type alloy MAGNEZIX® is the first absorbable alloy which obtained the CE marking of Medical Devices for medical applications within Europe [12]. Significance of the LAE442 alloy in the orthopaedic implant research has been proven by a comprehensive *in vivo* study, in which degradation behaviour of intramedullary interlocked nailing system implanted in an adult sheep for 24-week period was investigated [9]. After thorough investigation of implant volume development, *ex vivo* mechanical and histological examinations and elemental analyses of alloying elements in inner organs, the authors concluded that the extruded LAE442 alloy can be considered as a suitable degradable implant material. Additionally, beneficial effect of grain refinement on the *in vivo* corrosion of the LAE442 alloy was demonstrated after implantation of a single extruded and a double extruded material into rabbits [10].

As mentioned, decrease of the degradation rate of the LAE442 alloy was observed after subsequent extrusion, which led to decrease of the grain size and more uniform distribution of secondary phases in the material. It was reported that even further improved grain refinement could be achieved in the LAE442 alloy after subsequent equal channel angular pressing (ECAP) [13]. Uniform distribution of equiaxed grains of ~1.5 μm in diameter and much more uniform distribution of secondary phases was observed after 12 passes through ECAP. ECAP was already found to be an effective method to increase corrosion resistance of different magnesium alloys [14–16]. Therefore, further increase of the corrosion resistance of the LAE442 alloy is expected by comparison to the extruded samples. Moreover, substantial increase of the yield strength was observed in the fine-grained samples of the LAE442 alloy after ECAP [17].

Increase in mechanical strength could have beneficial effect for minimizing the implant size, which is important in particular applications. Furthermore, substantial grain refinement was found to have a positive effect on the fatigue resistance, which was found to be possibly insufficient in the extruded samples of the LAE442 alloy [18]. Therefore, the ECAP processing of LAE442 alloy may advance degradable properties of implant even further. To the best of our knowledge, the present study is the first one that aims to investigate the effect of ECAP on the *in vitro* degradation behaviour of the LAE442 magnesium alloy.

2 Experimental methods

2.1 Material

The investigated material was an extruded magnesium alloy LAE442 with the composition of 4.03wt.% Li – 3.56wt.% Al – 0.76wt.% La – 0.44wt.% Nd – 1.26wt.% Ce – 0.15wt.% Ca – 0.18wt.% Mn – < 0.0001 wt% Fe – <0.002 wt% Cu – <0.0002 Ni and balance Mg. Extrusion was performed at 350°C with an extrusion ratio of 22. Billets with the dimensions of 10x10x100 mm^3 were machined from the extruded bars and processed by ECAP. The ECAP processing direction was parallel to the extrusion direction. The processing was performed up to twelve passes (12P) following route B_C [19] in the temperature range of 185-230°C and ram speed of 5-10 $mm \cdot min^{-1}$. The angle Θ between two intersecting channels and the corner angle Ψ of the ECAP die were 90° and 0°, respectively. The samples of LAE442, which were extruded only, are designated Ex and the samples of LAE442, which were extruded and subsequently processed by ECAP, are designated 12P throughout the article.

2.2 Microstructure analysis

Microstructure of the specimens and corrosion layers after corrosion exposure were observed by scanning electron microscope (SEM) Zeiss AURIGA equipped by electron back scattered

diffraction (EBSD) detector and energy-dispersive X-ray spectroscopy (EDS). Samples for microstructure observation were mechanically polished down to 50 nm alumina solution. Additional ion polishing was performed for EBSD specimens using Gatan PIPS™.

2.3 Corrosion in NaCl

Initial corrosion resistance of the studied samples was investigated by electrochemical impedance spectroscopy (EIS). The measurement was performed using three-electrode setup and controlled by the potentiostat AUTOLAB 120N. Samples were cut perpendicular to the processing direction and exposed surface was ground with SiC1200 (15 μm) prior to each measurement. The measurement was performed in 0.1M NaCl solution after 5 minutes of stabilization. EIS tests were executed at room temperature in the frequency range of 100 kHz-20 mHz with 10mV amplitude with respect to the open circuit potential (OCP). Additional rotation of 1000 rpm was introduced to obtain better homogenization of the measurement. At least five measurements were performed for each sample/condition.

Hydrogen evolution was measured in 0.1M NaCl solution at room temperature for one week of immersion. Samples with dimensions 8x8x3 mm^3 were cut from the extruded and 12P bars. Subsequently they were ground (SiC1200, 15 μm) in ethanol in order to remove naturally occurring corrosion layer, measured and weighted.

2.4 Corrosion in biological media

Corrosion performance in biological media was investigated in Kirkland's biocorrosion medium (KBM, prepared according to [3] and buffered with $NaHCO_3$,), in KBM+10% FBS, in MEM (Sigma no. M0446) and MEM + 10% FBS. The ionic composition of both media in comparison with human plasma is given in Table 1. Samples with dimensions of 6x6x1.5 mm^3 were cut from extruded and 12P bars. Before the tests, samples were ground (SiC1200, 15 μm)

in ethanol in order to remove naturally occurring corrosion layer, measured, weighted and sonicated two times for 15 min in 96% ethanol. Three and two replicates of each sample type were used for corrosion rate determination and for corrosion layer examination, respectively. Samples were immersed into 40 ml ($S/V \approx 2.8$ mm^2/ml, i.e. $V/S = 36$ ml/cm^2) of media in falcon tubes with vented caps (Corning) and incubated in 5% CO_2 atmosphere at 37 °C on an orbital shaker for 14 days.

Table 1: Ionic concentrations of KBM prepared according to [3] and of MEM+10% FBS in comparison with human plasma.

medium	KBM	MEM	Human plasma
component	concentration [mmol/l]		
Cl^-	102.5	126.9	103
Na^+	120.3	143.6	142
Ca^{2+}	2.5	1.8	2.5
K^+	5.1	5.4	5.0
Mg^{2+}	0.5	0.8	1.5
HPO_4^{2-}	0.9	1.0	1.0
SO_4^{2-}	0.5	0.8	0.5
HCO_3^{2-}	26.2	26.2	22-30
glucose	5.0	5.6	5.0

After 14 days, the medium was removed and concentration of released Mg was measured using Atomic absorption spectrometer (AAS, Varian 220), while the pH of media was also recorded. Samples were immersed into a mixture of H_2CrO_4, $AgNO_3$ and $BaSO_4$ for 60 minutes at room temperature in order to remove the corrosion products. After drying, samples were weighted.

Corrosion rate (CR) was determined from the mass loss and was expressed in mg/cm^2/day. The corrosion rate was calculated using following formula (1):

$$CR = \frac{\Delta m}{A \times t} \quad (1)$$

CR: corrosion rate (mg/cm^2/day)

Δm: weight change in milligrams

A: surface area in cm^2

t: immersion time in days

2.5 *In vitro* cytotoxicity testing

In vitro cytotoxicity of extracts (indirect test) was tested according to ISO 10993-5 standard. Samples (6x6x1.5 mm) were sterilized in ethanol for 2 hours and then dried. Various surface-to-volume ratios and periods of incubation were used. In the first case, samples were immersed into 1 ml (S/V = 100 mm^2/ml) of cultivation media (MEM, Sigma M0446) without FBS, which is a surface-to-volume ratio closer to that recommended in ISO 10993-12 standard. Samples were agitated on an orbital shaker (125 rpm) at 37°C for 1 day. Thereafter, the extracts were centrifuged (5 min, 1,500 x g), supplemented with 10% FBS and immediately used for cytotoxicity testing. Three samples from each type (Ex and 12P) were used. Meanwhile, L929 cells (murine fibroblasts, ATCC® CCL-1™) were seeded into 96-well plates (100 µl/well) in the density of 1×10^5 cells/ml and incubated at 37 °C for 24 h in MEM + 10% FBS to allow cell adhesion. Thereafter, medium was replaced by the extracts in MEM medium with 10% FBS. MEM with 10% FBS only was used as a negative control.

In the second case, the conditions more were appropriate for magnesium alloys – i.e. higher amount of media for extraction and longer extraction time to simulate prolonged exposition of the samples in the body. Therefore, samples were immersed into 6 ml (S/V = 17 mm^2/ml) of cultivation media (MEM, Sigma M0446) supplemented with 5% FBS and agitated on an orbital

shaker (125 rpm) at 37 °C for 3 and also for 7 days. Decreased concentration of FBS was chosen according to ISO 10993-5 (higher concentration of FBS can mask the toxicity of the extracted substances). Three samples from each type (Ex and 12P) were used. Thereafter, the extracts were immediately used for cytotoxicity testing. Meanwhile, L929 cells were seeded into 96-well plates in the density of 1×10^5 cells/ml or 0.4×10^5 cells/ml and incubated at 37 °C for 24 h in MEM + 10% FBS to allow cell adhesion. Thereafter, medium was replaced by the extracts in MEM medium with 5% FBS. MEM with 5 % FBS only was used as a negative control.

The evaluation of the test was the same in both cases. After one and four days of incubation with the extracts, the cells were washed with phosphate buffer saline (PBS) and incubated with WST-1 reagent (5 % WST-1 in MEM without phenol red) for 2.5 hours. The yellow formazan product created by metabolic reduction was photometrically quantified using an ELISA reader at the absorption wavelength of 450 nm. Cytotoxic effect was depicted as a decrease in metabolic activity compared to the negative control. Cytotoxic measurement was done in 6 replicates for each sample. The limitary value of cytocompatibility was set as 70 % of metabolic activity of the untreated control (ISO 10993-5).

The results from corrosion studies in various media for the samples after extrusion and after additional ECAP processing were compared using ANOVA followed by Tukey's honest significance test in R software. A P-value < 0.05 was considered significant.

3 Results

3.1 Microstructure

EBSD micrographs of the investigated alloy after extrusion and twelve passes through ECAP are presented in Fig. 1. The initial microstructure of the extruded material was formed by fully recrystallized equiaxed grains with the average grain size of 21 μm in diameter. The severe plastic deformation introduced to the material during processing through ECAP resulted in

substantial grain refinement. Homogenous microstructure with uniform distribution of fine grains with average grain size of 1.7 µm was observed in the case of 12P sample. Thorough characterization of the microstructure evolution, together with detailed analysis of the secondary phases, of the LAE442 alloy processed by ECAP is shown elsewhere [13]. Nevertheless, substantial fragmentation and homogenization of distribution of the secondary phase particles within the matrix after ECAP should be noted, as depicted in Fig. 2.

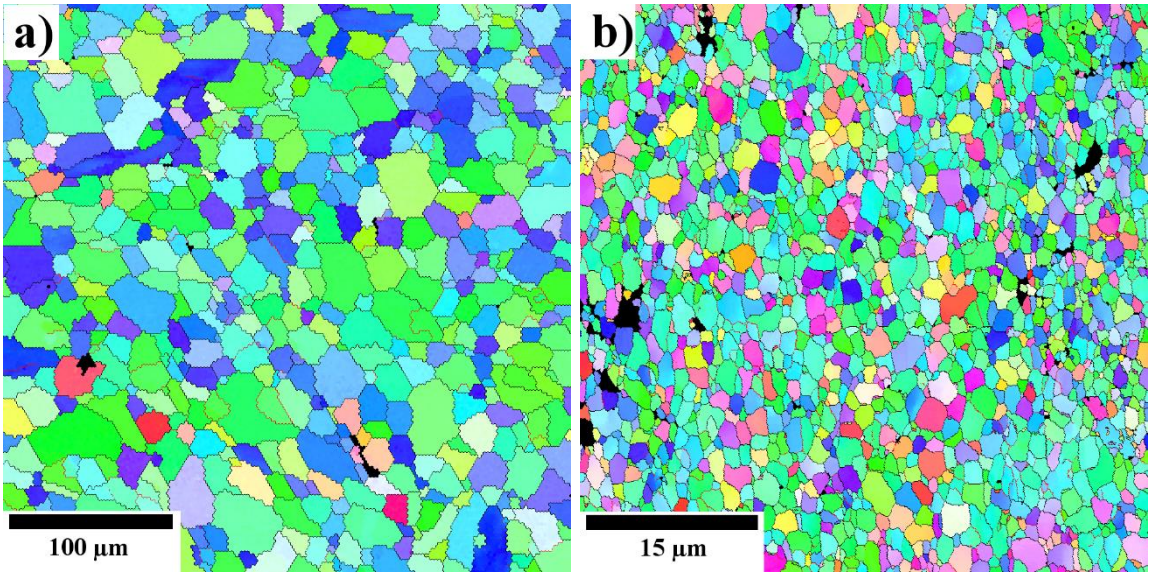

Fig. 1: EBSD micrographs of a) LAE442 Ex and b) LAE442 12P.

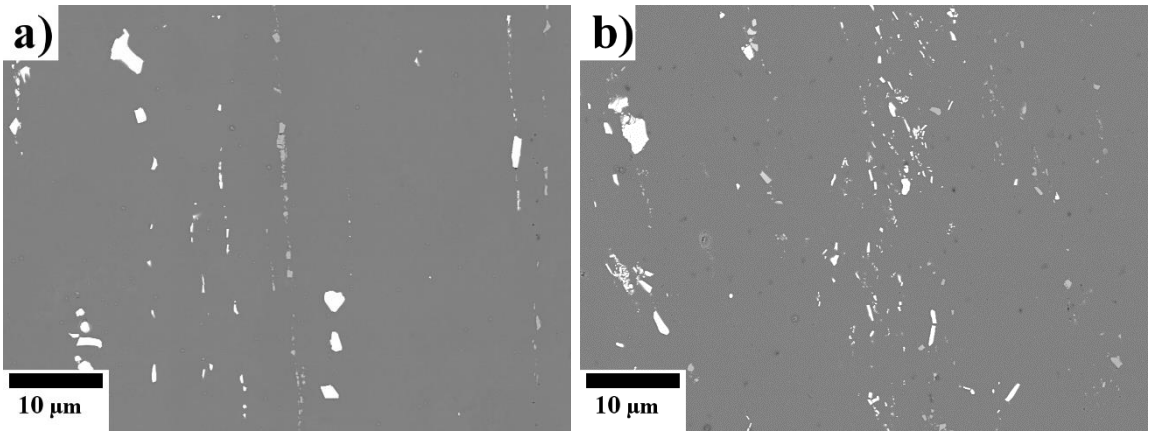

Fig. 2: Secondary phase particles distribution in a) LAE442 Ex and b) LAE442 12P (SEM, plane parallel to extrusion and ECAP direction).

3.2 Corrosion in NaCl

Effect of ECAP processing on the degradation behaviour of the LAE442 alloy was first investigated in 0.1M NaCl salt solution. The initial corrosion attack after 5 minutes of immersion was studied by EIS. The results are shown in the form of Bode plot as Fig. 3. The resulting values of total polarization resistance R_P were calculated as 142 ± 4 Ω·cm^2 and 202 ± 14 Ω·cm^2 for the extruded and 12P samples, respectively. The analysis of EIS data is shown in detail elsewhere [16]. Corrosion resistance resulting from EIS analysis was found to be much higher in 12P sample than in the Ex one. Higher corrosion resistance of the 12P sample in the 0.1M NaCl solution was observed also using hydrogen evolution measurement, as depicted in Fig. 4. This method was employed in order to observe evolution of the degradation rate over a one-week immersion. After one day of incubation period, volume of evolved hydrogen as a function of time was linear in both samples. Corrosion rate calculated from the linear part of the plot was 2.87±0.03 mg/cm^2/day and 2.49±0.02 mg/cm^2/day for the Ex and 12P samples, respectively.

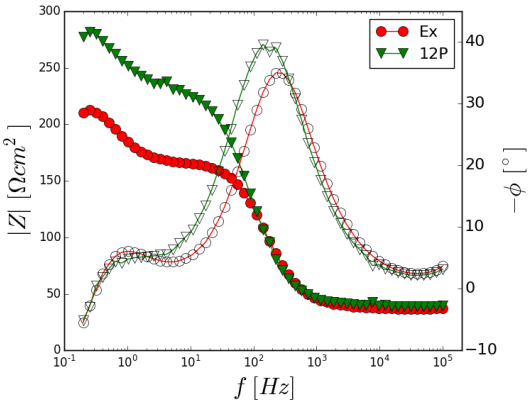

Fig. 3: Bode plots for the extruded and 12P sample, measured in 0.1M NaCl solution after 5 min of stabilization (full symbols – magnitude, empty symbols – phase angle).

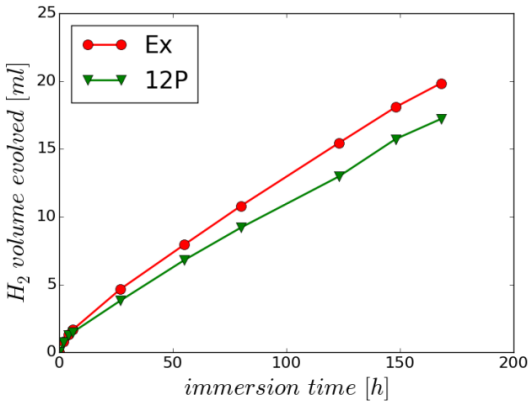

Fig. 4: Volume of hydrogen gas evolved as a function of immersion time in 0.1M NaCl solution.

3.3 Corrosion in biological media

In order to investigate the degradation rate in biological media, four types of solutions were used. KBM was chosen as a simulated body fluid (SBF) because, as mentioned in [3], it closely reflects ionic composition of the human plasma, especially concentration of Cl^- (contrary to other SBFs). Minimal essential medium (MEM) + 10% FBS was chosen as a cultivation medium and also used for *in vitro* cytotoxicity testing of the investigated samples. In order to study the influence of FBS, KBM + 10% FBS and MEM without FBS was also used. Both Ex and 12P samples were immersed into all solutions for 14 days. Afterwards, corrosion rate from mass loss was calculated. The results are presented in Fig. 5. The lowest degradation rate was found for 12P samples immersed in KBM+10% FBS. Importantly, the 12P samples had lower corrosion rate than Ex samples in all investigated media. It is important to note that after the immersion period, pH of each solution was below 7.6 for all tested samples and experimental setups.

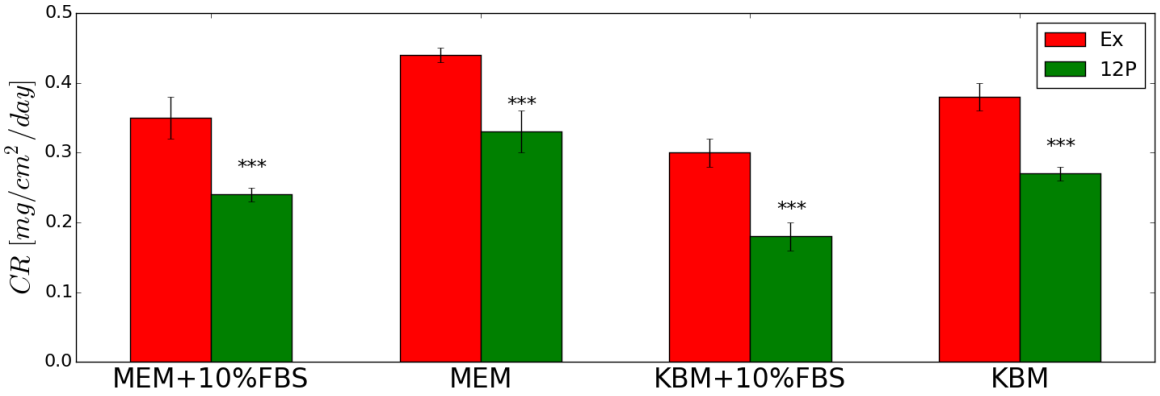

Fig. 5: Corrosion rate of LAE442 calculated from mass loss [mg/cm^2/day] after 14 days in 40 ml of media (KBM or MEM, with or without 10% FBS) in 5% CO_2 (error bars represent standard deviation, *** stands for $p < 0.001$).

3.4 Analysis of the corrosion layer morphology and composition

To better understand the reason for the differences in the degradation rate between investigated samples and different media, SEM images of the surfaces after the immersion were taken, see Fig. 6. The major difference in the observed corrosion layers formed on Ex and 12P samples was between immersion in KBM and other media. The samples immersed in KBM had rough surface with advanced disintegration, while in the other media, the corrosion layers had a dry, cracked earth structure. Generally, there was a major difference between the Ex and the 12P sample. The surface layers formed on 12P samples were more compact after corrosion in all media. In KBM, this difference is primarily due to deeper and more pronounced cracks in the extruded sample. In MEM, we observed advanced disintegration of the surface layer formed on the Ex sample contrary to the 12P sample. In case of both media with FBS addition, the difference between the extruded and 12P sample is mainly due to significantly higher density of cracks of the compact surface layer observed on the sample Ex.

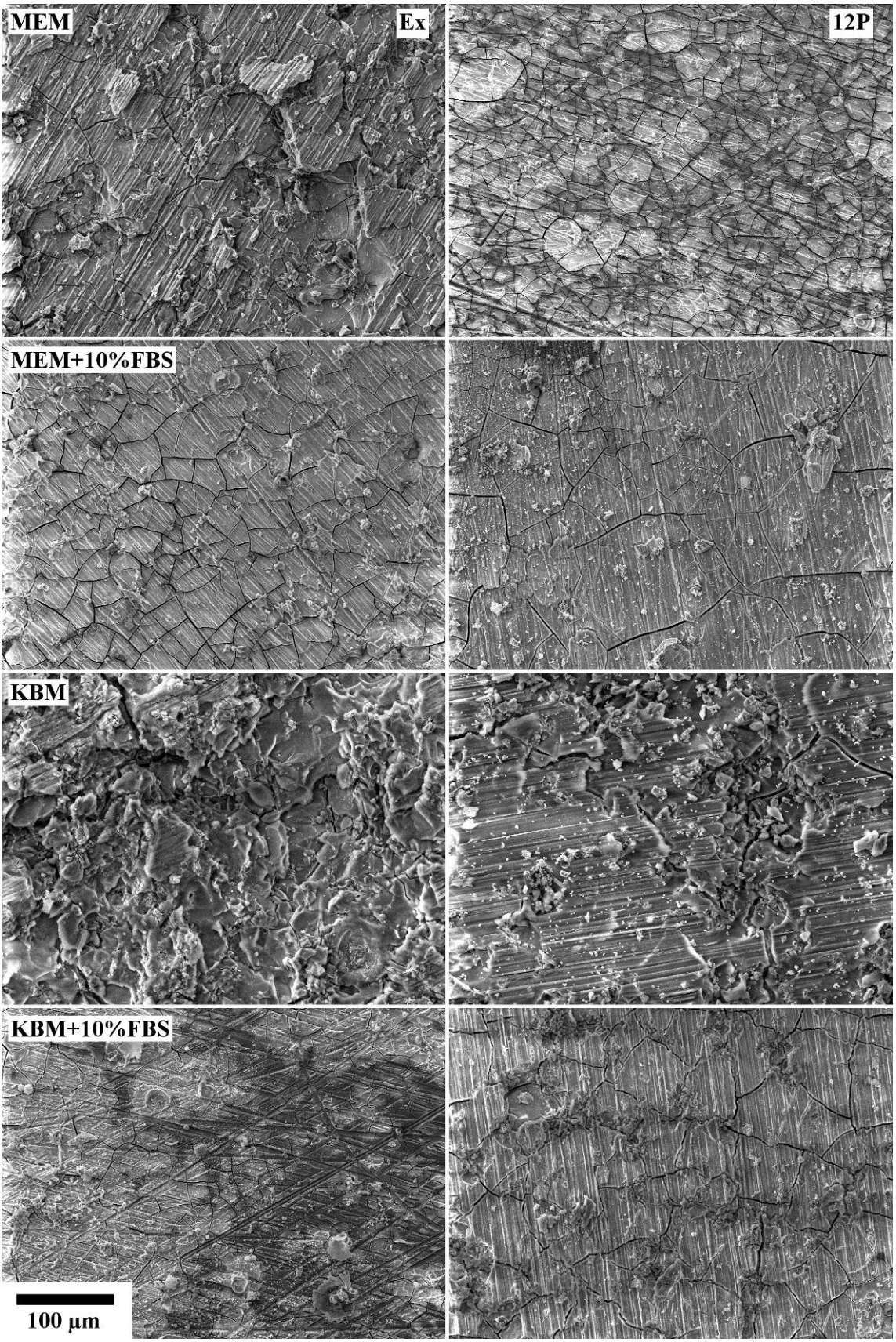

Fig. 6: Corrosion layer formed on the surface of the investigated samples after 14-days immersion in different biological media.

Not only the morphology of the corrosion layers formed in KBM and the other media were different, but there were also significant differences in their composition. Substantially higher content of Mg was observed in the layer formed in KBM, while in the other media, high content of Ca and P was measured. Calcium phosphate (CaP) compounds preferentially nucleates on $Mg(OH)_2$ [20], therefore differences between Mg and Ca+P concentration indicates a limited stability of CaP on the samples immersed in KBM media but much better stability in all other media. In MEM, comparable ratio between $Mg(OH)_2$ and CaP was observed. Composition of the corrosion layer was quite homogeneous through the surfaces of all studied samples, and there was no significant difference between extruded and 12P sample immersed in the same media. Table 2 shows composition difference between the corrosion layers formed on 12P samples immersed in different media.

Table 2: Elemental composition of the corrosion layers formed on the 12P samples after 14 days of immersion in different media.

at.%	KBM	KBM+10%FBS	MEM	MEM+10%FBS
O	61.6 ± 0.4	58.8 ± 0.2	59.7 ± 0.6	58.5 ± 0.7
Na	1.8 ± 0.3	2.0 ± 0.1	1.2 ± 0.2	1.4 ± 0.3
Mg	16.0 ± 0.4	8.0 ± 0.1	11.7 ± 0.8	7.5 ± 0.3
Al	7.3 ± 0.1	2.4 ± 0.1	3.3 ± 0.3	2.4 ± 0.3
P	6.8 ± 0.2	13.1 ±0.1	11.4 ± 0.3	13.3 ± 0.6
Cl	0.5 ± 0.1	0.2 ± 0.1	0.4 ± 0.1	0.1 ± 0.1
Ca	6.0 ± 0.3	15.7 ± 0.1	12.3 ± 0.6	16.6 ± 0.3

3.5 *In vitro* cytotoxicity testing

Metabolic activity of the L929 cells was not altered after exposure to the extracts of tested samples (Fig. 7); moreover, relative cell viability was far above 70 % limit stated in ISO standard. There were no differences in the cell response using various extraction media, extraction volumes, extraction periods or cultivation periods. Most importantly, there was no difference in cytotoxicity between the samples before and after ECAP processing. We can therefore assume that the cytocompatibility of LAE442 alloy in extruded state is sufficient and that additional ECAP processing has no adverse effects on the cytocompatibility of this alloy.

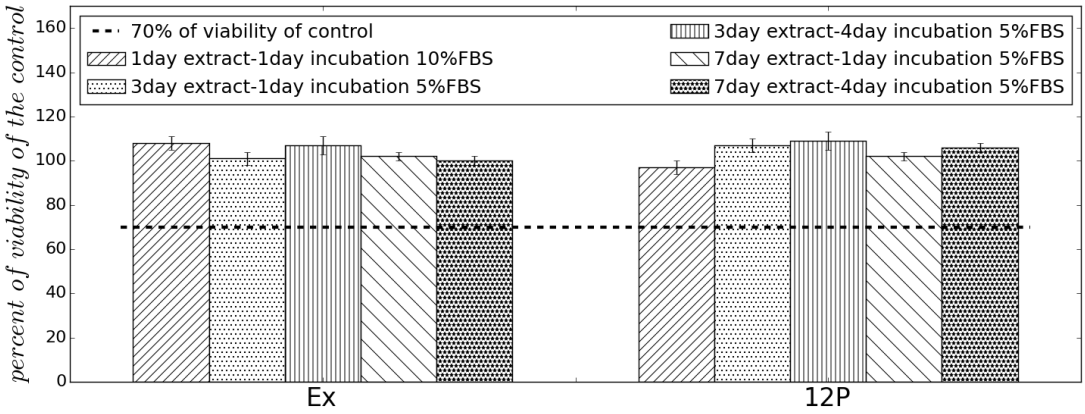

Fig 7: Metabolic activity of L929 after 1-day or 4-day exposition to LAE442 extracts prepared using various media and extraction periods. Dashed line stands for the cut-off between non-toxic and toxic response. Error bars represent sample standard deviation from six replicates.

4 Discussion

4.1 Corrosion in NaCl

Increase in the corrosion resistance after ECAP was already observed in a number of magnesium alloys, as mentioned above. The major reason was found to be a combination of better distribution of corrosion layer stabilizing alloying elements through the material, together

with reduced grain size [16,21]. The decrease in the grain size has two major impacts on the corrosion behaviour. Higher density of lattice defects leads to an increased severity of the corrosion attack, but it also leads to a decrease in the mismatch between the corrosion layer and matrix. Therefore, a decrease in the corrosion layer cracking occurs [22]. As a result, more stable protective surface films form faster [16]. Aluminium contained in the investigated alloy is an element that could positively affect corrosion resistance, as shown previously [21,23–25]. Aluminium oxides tend to fill pores of the porous $Mg(OH)_2$ corrosion layer and increase its protection ability. Nevertheless, it should be noted that the concentration of aluminium must exceed certain threshold level in order to enhance the corrosion resistance after ECAP [16]. Similar functionality of lithium was also previously reported. Li(OH) corrosion products increased corrosion resistance due to the deposition within porous surface layer [26–29]. However, detection of Li(OH) is experimentally challenging and its deposition within the corrosion layer of the LAE442 alloy has not been proven yet. Nevertheless, the increase of the polarization resistance of the LAE442 alloy after ECAP was much higher than the increase previously observed in the lithium free AE42 alloy, which was measured under the same conditions [16]. Therefore, faster formation of corrosion layer stabilized by Al oxides together with Li hydroxides in 12P sample explains higher corrosion resistance achieved in the LAE442 alloy compared to the AE42 alloy. The significant increase of the corrosion resistance after ECAP in the LAE442 alloy was therefore achieved by better distribution of Al-rich secondary phases due to fragmentation (Fig. 2), similar as observed in AE42 alloy, formation of fine distribution of aluminium rich particles within the matrix [13] and possibly the enhancing effect of Li. Combination of all these factors resulted in faster formation of more stable protective surface film.

Higher corrosion resistance of 12P sample was observed not only immediately after the immersion, as demonstrated by the hydrogen evolution measurement. The linear character of

both plots indicates uniform degradation in both investigated samples after one day of immersion. Higher corrosion rate of extruded sample is directly visible from higher volume of evolved hydrogen. This hypothesis is supported also by the values of the calculated corrosion rates. The higher corrosion resistance found in 12P sample together with the uniform degradation in 0.1M NaCl solution is an important information that predestines this material for subsequent corrosion tests in biological media.

4.2 Corrosion in biological media

Degradation behaviour in biological media was investigated using immersion tests and corrosion rate was calculated form mass loss evaluation. Corrosion rate was significantly ($p < 0.01$) lower in the presence of 10% FBS for both types of samples in both media used (KBM and MEM). 10% FBS corresponds approximately to the protein concentration of 3.2-7 mg/ml. Our observation is in a good agreement with the published data [30] where lower corrosion rate of pure magnesium in the presence of FBS was observed. Kirkland and Birbilis observed even three times lower corrosion rates of various magnesium alloys in MEM + 10% FBS compared to sole MEM [3]. This can be explained by the formation of more uniform, thicker and more protective layer resulting from protein adsorption [3] since proteins readily interact with Mg divalent ions [31]. More stable and protective layer was also observed by SEM of samples immersed in both media with FBS, see Fig 6. Adding 10% of FBS into the KBM resulted in a significant change of the corrosion layer character, while in the case of the MEM, the difference was not so pronounced. Nevertheless, in the case of both media EDX analysis showed (Table 2) that the addition of FBS led to increase of stability of CaP on the surface, which has higher protection ability than the sole $Mg(OH)_2$. Therefore, it is assumed that higher stability of the corrosion layer formed in both media with FBS led to higher corrosion resistance of the samples.

Corrosion rate was significantly ($p < 0.05$) lower in KBM than in MEM. This is probably caused by slightly higher concentration of Cl^- in MEM (Table 1). As mentioned in [3], higher concentration of Cl^- accelerates the corrosion rate of Mg alloys.

The most important result is that the corrosion rate after ECAP processing was significantly ($p < 0.001$) lower in all used media, which is consistent with results obtained by EIS and H_2 evolution in NaCl. Investigation of the corrosion layers by SEM has shown higher stability of the corrosion layer formed on 12P samples in all used media, when compared to the extruded ones. Therefore, microstructure of the studied samples had a direct impact on the stability of the corrosion layer, as discussed above in chapter 4.1. After ECAP, the density of cracks substantially decreased. This is in accordance with the previous results, which point out that substantial grain refinement leads to a decrease of the mismatch between corrosion layer and matrix, resulting in increase of the corrosion layer protection ability [21].

The pH values of media after immersion period were below 7.6 for all tested samples and solutions. Thus, crucial requirement for maintaining the physiological pH range (7.4-7.6), as recommended in [3], was complied. This is important, because higher pH generally results in more stable and protective CaP surface film that could significantly decrease corrosion rate of the studied material, and subsequently affect the results.

4.3 *In vitro* cytotoxicity testing

Under the selected conditions, we observed no cytotoxic effect of extracts prepared from LAE442 after both types of processing. Our results indicate that even the extruded state of LAE442 alloy has a sufficient cytocompatibility, which is in agreement with previously published observation [32] where the cytocompatibility of extruded magnesium alloys with Li, Al and RE was studied. The relative viability of ECV304 and VSMC cells after one-day incubation with extracts of Mg-3.5Li-4Al-2RE exceeded 70%. In another study, *in vitro*

cytotoxicity tests with an extruded LAE442 alloy were performed [18]. Only slightly reduced viability (70% viability of the control) of L929 cells after incubation with 100% (undiluted) extracts of the extruded LAE442 alloy was observed. This could be caused by a smaller extraction volume used. As mentioned in the introduction, as-cast and extruded LAE442 alloy were also tested *in vivo* and were clinically well tolerated. Therefore, a positive influence of ECAP processing on *in vivo* behaviour can be assumed.

5 Conclusions

We have demonstrated that the ECAP processing decelerates the corrosion rate of the LAE442 magnesium alloy not only during short-term electrochemical experiments in NaCl, but also in longer-term experiments in more complex biological media, such Kirkland's biocorrosion medium and Minimal essential medium, both with and without the addition of 10% FBS. Thus, it is concluded that ECAP processing can be used to improve corrosion resistance of the LAE442 magnesium alloy as a material for temporary orthopaedic implants. These results, together with our successful *in vitro* cytotoxicity tests, let us to conclude that future work should focus on *in vivo* corrosion testing and biocompatibility of LAE442 after ECAP.

6 Acknowledgement

The present work is a part of the Czech Science Foundation project 14-13415S, Operational Programme CZ.2.16/3.1.00/24503 and NPU I LO1601 - No.: MSMT-43760/2015. B.H. acknowledges the financial support for Slovak Research and Development Agency under the project No. APVV-14-0772 and for Slovak Scientific Grant Agency under the project No.1/0720/14. Authors wish to thank Dr. Eva Mištová for AAS measurements.

7 References

[1] Y.F. Zheng, X.N. Gu, F. Witte, Biodegradable metals, Mater. Sci. Eng. R Rep. 77 (2014) 1–34. doi:10.1016/j.mser.2014.01.001.

[2] F. Witte, N. Hort, C. Vogt, S. Cohen, K.U. Kainer, R. Willumeit, F. Feyerabend, Degradable biomaterials based on magnesium corrosion, Curr. Opin. Solid State Mater. Sci. 12 (2008) 63–72. doi:10.1016/j.cossms.2009.04.001.

[3] N.T. Kirkland, N. Birbilis, Introduction to Magnesium Biomaterials, in: Magnes. Biomater., Springer International Publishing, 2014: pp. 1–12. http://link.springer.com/chapter/10.1007/978-3-319-02123-2_1 (accessed March 19, 2015).

[4] F. Witte, V. Kaese, H. Haferkamp, E. Switzer, A. Meyer-Lindenberg, C.J. Wirth, H. Windhagen, In vivo corrosion of four magnesium alloys and the associated bone response, Biomaterials. 26 (2005) 3557–3563. doi:10.1016/j.biomaterials.2004.09.049.

[5] F. Witte, J. Fischer, J. Nellesen, H.-A. Crostack, V. Kaese, A. Pisch, F. Beckmann, H. Windhagen, In vitro and in vivo corrosion measurements of magnesium alloys, Biomaterials. 27 (2006) 1013–1018. doi:10.1016/j.biomaterials.2005.07.037.

[6] F. Witte, J. Fischer, J. Nellesen, C. Vogt, J. Vogt, T. Donath, F. Beckmann, In vivo corrosion and corrosion protection of magnesium alloy LAE442, Acta Biomater. 6 (2010) 1792–1799. doi:10.1016/j.actbio.2009.10.012.

[7] A. Krause, N. von der Höh, D. Bormann, C. Krause, F.-W. Bach, H. Windhagen, A. Meyer-Lindenberg, Degradation behaviour and mechanical properties of magnesium implants in rabbit tibiae, J. Mater. Sci. 45 (2010) 624–632. doi:10.1007/s10853-009-3936-3.

[8] M. Thomann, C. Krause, D. Bormann, N. von der Höh, H. Windhagen, A. Meyer-Lindenberg, Comparison of the resorbable magnesium alloys LAE442 und MgCa0.8 concerning their mechanical properties, their progress of degradation and the bone-implant-contact after 12 months implantation duration in a rabbit model, Mater. Werkst. 40 (2009) 82–87. doi:10.1002/mawe.200800412.

[9] C. Rössig, N. Angrisani, P. Helmecke, S. Besdo, J.-M. Seitz, B. Welke, N. Fedchenko, H. Kock, J. Reifenrath, In vivo evaluation of a magnesium-based degradable intramedullary nailing system in a sheep model, Acta Biomater. 25 (2015) 369–383. doi:10.1016/j.actbio.2015.07.025.

[10] B. Ullmann, J. Reifenrath, J.-M. Seitz, D. Bormann, A. Meyer-Lindenberg, Influence of the grain size on the in vivo degradation behaviour of the magnesium alloy LAE442, Proc. Inst. Mech. Eng. [H]. 227 (2013) 317–326.

[11] N. Angrisani, J. Reifenrath, F. Zimmermann, R. Eifler, A. Meyer-Lindenberg, K. Vano-Herrera, C. Vogt, Biocompatibility and degradation of LAE442-based magnesium alloys after implantation of up to 3.5 years in a rabbit model, Acta Biomater. 44 (2016) 355–365. doi:10.1016/j.actbio.2016.08.002.

[12] H. Windhagen, K. Radtke, A. Weizbauer, J. Diekmann, Y. Noll, U. Kreimeyer, R. Schavan, C. Stukenborg-Colsman, H. Waizy, Biodegradable magnesium-based screw clinically equivalent to titanium screw in hallux valgus surgery: short term results of the first prospective, randomized, controlled clinical pilot study, Biomed. Eng. Online. 12 (2013) 62. doi:10.1186/1475-925X-12-62.

[13] P. Minárik, R. Král, J. Pešička, S. Daniš, M. Janeček, Microstructure characterization of LAE442 magnesium alloy processed by extrusion and ECAP, Mater. Charact. 112 (2016) 1–10. doi:10.1016/j.matchar.2015.12.002.

[14] J. Jiang, A. Ma, N. Saito, Z. Shen, D. Song, F. Lu, Y. Nishida, D. Yang, P. Lin, Improving corrosion resistance of RE-containing magnesium alloy ZE41A through ECAP, J. Rare Earths. 27 (2009) 848–852. doi:10.1016/S1002-0721(08)60348-8.
[15] B. Hadzima, M. Janecek, M. Bukovina, R. Kral, Electrochemical properties of fine-grained AZ31 magnesium alloy, Int. J. Mater. Res. 100 (2009) 1213–1216. doi:10.3139/146.110186.
[16] P. Minárik, R. Král, M. Janeček, Effect of ECAP processing on corrosion resistance of AE21 and AE42 magnesium alloys, Appl. Surf. Sci. 281 (2013) 44–48. doi:10.1016/j.apsusc.2012.12.096.
[17] P. Minárik, R. Král, J. Čížek, F. Chmelík, Effect of different c/a ratio on the microstructure and mechanical properties in magnesium alloys processed by ECAP, Acta Mater. 107 (2016) 83–95. doi:10.1016/j.actamat.2015.12.050.
[18] M. Krämer, M. Schilling, R. Eifler, B. Hering, J. Reifenrath, S. Besdo, H. Windhagen, E. Willbold, A. Weizbauer, Corrosion behavior, biocompatibility and biomechanical stability of a prototype magnesium-based biodegradable intramedullary nailing system, Mater. Sci. Eng. C. 59 (2016) 129–135. doi:10.1016/j.msec.2015.10.006.
[19] K. Nakashima, Z. Horita, M. Nemoto, T.G. Langdon, Development of a multi-pass facility for equal-channel angular pressing to high total strains, Mater. Sci. Eng. A. 281 (2000) 82–87. doi:10.1016/S0921-5093(99)00744-3.
[20] J.X. Yang, F.Z. Cui, Q.S. Yin, Y. Zhang, T. Zhang, X.M. Wang, Characterization and Degradation Study of Calcium Phosphate Coating on Magnesium Alloy Bone Implant In Vitro, IEEE Trans. Plasma Sci. 37 (2009) 1161–1168. doi:10.1109/TPS.2009.2016664.
[21] A. Pardo, M.C. Merino, A.E. Coy, R. Arrabal, F. Viejo, E. Matykina, Corrosion behaviour of magnesium/aluminium alloys in 3.5 wt.% NaCl, Corros. Sci. 50 (2008) 823–834. doi:10.1016/j.corsci.2007.11.005.
[22] N. Birbilis, K.D. Ralston, S. Virtanen, H.L. Fraser, C.H.J. Davies, Grain character influences on corrosion of ECAPed pure magnesium, Corros. Eng. Sci. Technol. 45 (2010) 224–230. doi:10.1179/147842209X12559428167805.
[23] M. Liu, P.J. Uggowitzer, A.V. Nagasekhar, P. Schmutz, M. Easton, G.-L. Song, A. Atrens, Calculated phase diagrams and the corrosion of die-cast Mg–Al alloys, Corros. Sci. 51 (2009) 602–619. doi:10.1016/j.corsci.2008.12.015.
[24] G. Wu, Y. Fan, H. Gao, C. Zhai, Y.P. Zhu, The effect of Ca and rare earth elements on the microstructure, mechanical properties and corrosion behavior of AZ91D, Mater. Sci. Eng. A. 408 (2005) 255–263. doi:10.1016/j.msea.2005.08.011.
[25] Y. Fan, G. Wu, C. Zhai, Influence of cerium on the microstructure, mechanical properties and corrosion resistance of magnesium alloy, Mater. Sci. Eng. A. 433 (2006) 208–215. doi:10.1016/j.msea.2006.06.109.
[26] J. Gui, T.M. Devine, Influence of lithium on the corrosion of aluminum, Scr. Metall. 21 (1987) 853–857. doi:10.1016/0036-9748(87)90336-X.
[27] J.P. Moran, E.A.J. Starke, G.E. Stoner, G.L.J. Cahen, Corrosion. 1986 (n.d.).
[28] M.C. Bloom, W.A. Fraser, M. Krulfeld, Corrosion of Steel in Concentrated Lithium Hydroxide Solution at 316 C, Corrosion. 18 (1962) 401–405. doi:10.5006/0010-9312-18.11.401.
[29] M.C. Bloom, M. Krulfeld, W.A. Fraser, Some Effects of Alkalis on Corrosion Of Mild Steel in Steam Generating Systems, Corrosion. 19 (1963) 327–330. doi:10.5006/0010-9312-19.9.327.
[30] A. Yamamoto, S. Hiromoto, Effect of inorganic salts, amino acids and proteins on the degradation of pure magnesium in vitro, Mater. Sci. Eng. C. 29 (2009) 1559–1568. doi:10.1016/j.msec.2008.12.015.

[31] C. Liu, Y. Xin, X. Tian, P.K. Chu, Degradation susceptibility of surgical magnesium alloy in artificial biological fluid containing albumin, J. Mater. Res. 22 (2007) 1806–1814. doi:10.1557/jmr.2007.0241.
[32] W.R. Zhou, Y.F. Zheng, M.A. Leeflang, J. Zhou, Mechanical property, biocorrosion and in vitro biocompatibility evaluations of Mg–Li–(Al)–(RE) alloys for future cardiovascular stent application, Acta Biomater. 9 (2013) 8488–8498. doi:10.1016/j.actbio.2013.01.032.